ChemComm

Cite this: *Chem. Commun.*, 2012, **48**, 8637–8639

www.rsc.org/chemcomm

COMMUNICATION

Benzothiazolium-functionalized tetraphenylethene: an AIE luminogen with tunable solid-state emission†

Na Zhao,[a] Zhiyong Yang,[a] Jacky W. Y. Lam,[a] Herman H. Y. Sung,[a] Ni Xie,[a] Sijie Chen,[a] Huimin Su,[b] Meng Gao,[a] Ian D. Williams,[a] Kam Sing Wong[b] and Ben Zhong Tang*[ac]

Received 26th May 2012, Accepted 10th July 2012
DOI: 10.1039/c2cc33780k

Melding a benzothiazolium unit with tetraphenylethene generates a new hemicyanine luminogen with aggregation-induced emission characteristics; the luminogen exhibits crystochromism and its solid-state emission can be repeatedly tuned from yellow or orange to red by grinding–fuming or grinding–heating processes due to the transformation from the crystalline to the amorphous state and *vice versa*.

Creation of efficient luminogenic materials is a hot research topic. Of particular interest are those luminogens with tunable and reversible emission in the solid state due to their potential applications in biotechnology and memory systems.[1] A problem associated with the emissions of most luminogenic materials in the solid state is aggregation-caused quenching (ACQ): during film formation, the dye molecules are located in close vicinity and are inclined to form aggregates, which favour the formation of detrimental species such as excimers.[2] In 2001, we found that some propeller-shaped molecules exhibit the phenomenon of aggregation-induced emission (AIE) which is exactly opposite to the ACQ effect.[3] Instead of quenching, aggregate formation has induced them to emit intensely. Since then, a variety of AIE luminogens have been prepared[4–6] and utilized in various applications.[7] Most of the AIE luminogens prepared so far, however, emit blue or green light. Few emitters with longer emission wavelengths have been prepared, possibly due to synthetic difficulty, though they suffer little interferences from optical absorption and light scattering.[8]

[a] *Department of Chemistry, Institute for Advanced Study, State Key Laboratory of Molecular Neuroscience, Institute of Molecular Functional Materials and Division of Biomedical Engineering, The Hong Kong University of Science & Technology (HKUST), Clear Water Bay, Kowloon, Hong Kong, China. E-mail: tangbenz@ust.hk*
[b] *Department of Physics, HKUST, Clear Water Bay, Kowloon, Hong Kong, China*
[c] *Department of Polymer Science & Engineering, Zhejiang University, Hangzhou, 310027, China*

† Electronic supplementary information available: Synthesis and characterization of **2** and **3**; crystal data for **1**, **1**·2/3 THF and **1**·EtOAc and their HOMO and LUMO energy levels; views of interactions between molecules in crystals of **1**; TEM and SEM images and ED patterns of amorphous and crystalline aggregates of **1**; change in the PL spectrum of **1** by repeated grinding–heating cycles; and XRD and DSC profiles of **1** at different aggregated states. CCDC 883789–883791. For ESI and crystallographic data in CIF or other electronic format see DOI: 10.1039/c2cc33780k

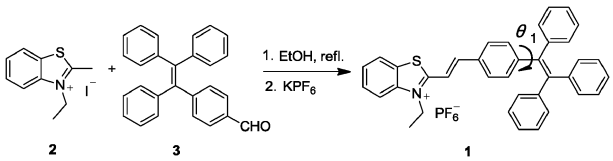

Scheme 1 Synthetic route to luminogen **1**.

Cyanine dyes have been widely used for fluorescent sensory applications for hundreds of years.[9] Recently, they have been successfully applied as nonlinear optical materials[10] and chemosensors[11] as their absorption and emission colour can easily reach the red and near infrared region. However, they suffer some drawbacks such as small Stokes shift and ACQ effect,[12] thus making realization of their full potential a daunting task.

To enlarge the family of AIE-active red emitters, in this communication, we generated a hemicyanine dye by attaching a benzothiazolium unit, a building block for cyanine dye, to tetraphenylethene (TPE), a typical AIE luminogen,[7b] through vinyl functionality (**1**; Scheme 1). Luminogen **1** inherits the AIE feature of TPE and emits at longer wavelength. Whereas many dye molecules show tunable light emission in the solution state, luminogen **1** exhibits crystochromism and its solid-state emission can be repeatedly tuned by grinding–fuming and grinding–heating processes, which are rarely reported in the AIE system.[13]

Luminogen **1** was synthesized as a yellow solid in a yield of 62% according to the synthetic route shown in Scheme 1. Detailed procedures for its synthesis and characterization can be found in the ESI.†

Crystals of **1** were obtained by slow evaporation of its DCM–ethanol, THF–hexane and DCM–ethyl acetate (EtOAc) mixtures and analyzed by single crystal X-ray diffraction. Their ORTEP drawings are shown in Fig. S1 (ESI†) and the crystal data are given in Table S1 (ESI†). Interestingly, the crystals grown from different solvent mixtures emit at different wavelengths with different efficiencies (Fig. S2, ESI† and Table 1). To gain insight into the distinct emission behavior of the crystals, we checked their geometric structures and packing arrangements. Due to the propeller-shaped TPE unit, all the crystals adopt a highly twisted conformation. The torsion angles (θ_1) between the bridged phenyl ring and the vinyl core of TPE in crystals of **1**, **1**·2/3 THF and **1**·EtOAc are 70.42°, 70.37° and 67.94°, respectively, suggesting that the molecular conjugation is in the order **1** < **1**·2/3 THF < **1**·EtOAc. This agrees well with their observed emission maximum,

Table 1 Photophysical properties, torsion angles and energy gaps of crystals of **1**[a]

Crystal	λ_{em} (nm)	Φ_F (%)	θ_1 (°)	ΔE (eV)
1	565	18.0	70.42	1.89
1·2/3 THF	578	28.2	70.37	1.83
1·EtOAc	591	43.6	67.94	1.79

[a] Abbreviations: λ_{em} = emission maximum, Φ_F = fluorescence quantum yield determined using a calibrated integrating sphere, ΔE = energy band gap determined using the B3LYP/6-31G(d) basis set.

in which crystals of **1**·EtOAc are the redder emitters. As shown in Fig. S3–S5 (ESI†), except weak π–π stacking interaction between the benzothiazolium units, multiple C–H···π and C–H···F hydrogen bonds and S···F interaction are observed in all crystals. Additional C–H···π and C–H···O hydrogen bonds that arise from interactions with the solvent molecules are also found in crystals of **1**·2/3 THF and **1**·EtOAc. These multiple bonds and interactions help further rigidify the molecular conformation, which reduces the energy loss through the nonradiative rotational relaxation channel and thus enhances the emission efficiency of **1**·2/3 THF and **1**·EtOAc. The HOMO and LUMO energy levels of the crystals were calculated using the 3LYP/6-31G* basis set and the results are given in Fig. S6 (ESI†). The HOMO of all crystals is dominated by the orbitals of the TPE unit, while the orbitals of the benzothiazolium component contribute mainly to the LUMO energy levels. The energy band gaps of **1**, **1**·2/3 THF and **1**·EtOAc are calculated to be 1.89, 1.83 and 1.79 eV, respectively, nicely correlating with their different emission colors. Clearly, the crystal emission of **1** can be tuned readily by solvent molecules, which is extraordinary, if not unprecedented in the AIE system.

Luminogen **1** absorbs at 440 nm in diluted THF solution (Fig. S2, ESI†) due to the intramolecular charge transfer (ICT) from the electron-donating TPE unit to the electron-accepting benzothiazolium unit.[14] Similar to TPE, luminogen **1** emits faint photoluminescence (PL) at 663 nm with a fluorescence quantum yield (Φ_F) of 3.66% when its diluted solution is photoexcited (Fig. 1A). When a small amount of water is added to the THF solution, the emission intensity as well as the Φ_F value becomes lower, presumably due to the ICT effect. The higher the water content, the lower the light emission and the Φ_F value because the solution polarity becomes higher progressively. Interestingly, at water fraction >90%, the mixture emits even more intensely and efficiently than pure THF solution. At 99% water content, the Φ_F value is 13.12%, which is more than 3-fold higher than that in pure THF solution. Clearly, **1** is AIE-active. We have hypothesized that restriction of intramolecular rotation (RIR) is the main cause for the AIE phenomenon, which blocks the nonradiative relaxation channel and populates radiative excitons.[15] Since **1** is not soluble in water, its molecules must have been aggregated in aqueous mixtures with high water fractions. However, at water fraction ≤90%, the ICT effect still dominates. Afterwards, the RIR process prevails, which turns **1** into a strong emitter.

Amusingly, the emission intensity and color of a freshly prepared 90% aqueous mixture change when standing at room temperature with time. As depicted in Fig. 1C, the PL spectrum initially peaks at 644 nm, which shifts progressively to 566 nm

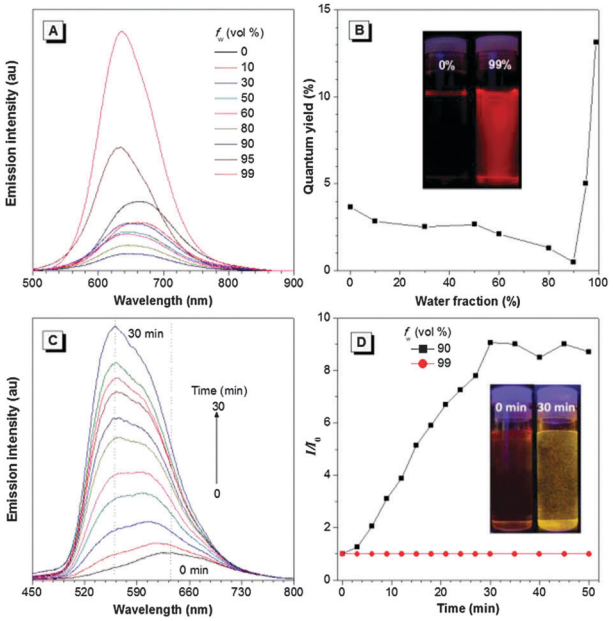

Fig. 1 (A) PL spectra of **1** in THF and THF–water mixtures with different water fractions (f_w). (B) Plots of fluorescence quantum yields *versus* the composition of the aqueous mixtures of **1**. (C) Change in the PL spectrum of **1** in 90% aqueous mixtures with time from 0 to 30 min. (D) Plot of I/I_0 value *versus* time in THF–water mixtures of **1** with 90 and 99% water contents. I_0 = emission intensity in pure THF solution. Solution concentration: 20 μM; excitation wavelength: 425 nm. Inset: photographs of **1** in (B) THF–water mixtures with f_w values of 0 and 90 vol% and (C) 90% aqueous mixture at different time intervals (0 and 30 min) taken under 365 nm UV illumination.

accompanied with a remarkable enhancement in the emission intensity. In contrast, such a phenomenon was not observed in the 99% aqueous mixture (Fig. 1D). Since the ultimate emission maximum is close to that of crystals, it is implied that the aggregates crystallize over time. This is supported by the TEM and SEM images and ED patterns shown in Fig. S7 (ESI†). The aggregates formed in the 90% aqueous mixture may possess a more loose structure than those in the THF–water mixture with 99% water fraction, which provides more free volume for the molecules to reorient and pack in a more ordered fashion. The unusual blue-shift observed in the crystalline phase, on the other hand, may be due to the conformation twisting of the aromatic rings of **1** in order to fit into the crystalline lattice. Without such constraint, the molecules in the amorphous phase may assume a more planar conformation and thus show a redder emission.

Mechanochromic luminescent materials have received considerable interest in recent years in view of their potential applications in camouflage and optical information storage systems.[13b] The crystals of **1** show strong yellow emission at 565 nm. Intriguingly, after gentle grinding using a pestle and a mortar, red powders are formed, which show red PL at 650 nm (Fig. 2 and 3A). After fuming with acetone vapor for 10 min, the initial (yellow) appearance is reinstalled (Fig. 3A). The conversion between yellow and red emission colors can be repeated many times without fatigue as these stimuli are nondestructive in nature (Fig. 3B). On the other hand, heating the ground sample at 150 °C for 10 min changes its colour from red to orange (Fig. 2 and Fig. S8A, ESI†).

Fig. 2 Switching the solid-state emission of **1** by repeated grinding–fuming and grinding–heating processes. The photographs were taken under 365 nm UV irradiation.

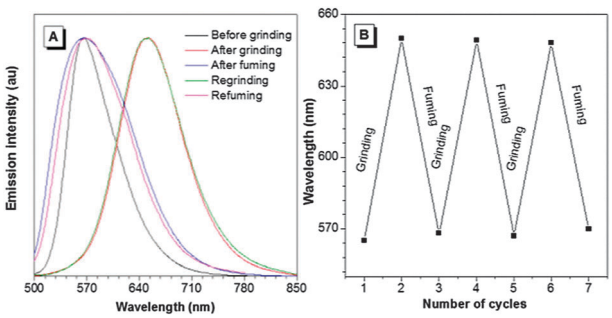

Fig. 3 (A) Change in the PL spectrum of **1** by grinding–fuming process. (B) Repeated switching of the solid-state fluorescence of **1** by repeated grinding and fuming cycles.

Again, such switching is reversible and suffers little wavelength-shift after many cycles (Fig. S8B, ESI†).

To gain insight into the mechanism for such a phenomenon, we analyzed **1** at different aggregated states by powder X-ray diffraction (XRD). The XRD diffractogram of the untreated sample exhibits many sharp diffraction peaks, indicative of its crystalline nature (Fig. S9A, ESI†). In contrast, the ground sample is amorphous as its diffractogram exhibits only a big, diffuse halo. When the red powders are thermally-treated or fumigated with solvent vapor, sharp diffraction peaks emerge again. This suggests that the amorphous powders crystallize upon solvent fumigation or thermal treatment. Now, it becomes clear that the mechanochromism observed in **1** is associated with the morphology change from the crystalline to the amorphous state and *vice versa*. It is noteworthy that the fumed sample shows much sharper peaks than the thermally-treated one, implying the stronger effect of solvent fumigation on the crystallization of **1** than the thermal process. This also explains why the red amorphous powders cannot be completely recovered as yellow-emissive crystals by the latter method.

Analysis by differential scanning calorimetry (DSC) also substantiates the above claim. The DSC curve of crystals of **1** recorded during the heating scan is basically a straight line parallel to the abscissa (Fig. S9B, ESI†). In contrast, an endothermic peak at 138 °C is detected in the ground sample. Thermogravimetric analysis shows that **1** exhibits a 5% weight loss at 280 °C. The peak at 138 °C thus should not stem from the decomposition of the molecule or its glass-transition temperature as such thermal transition involves only a small enthalpy change. Instead, it is more likely to be associated with the crystallization of the luminogen. No signals are detected in thermally-treated and fumed samples as they are crystalline.

In summary, an AIE hemicyanine dye was synthesized by incorporation of a benzothiazolium unit into TPE through vinyl functionality. Luminogen **1** exhibits crystochromism and its crystals emit stronger and bluer PL than its amorphous aggregates. Its solid-state emission can be tuned reversibly from yellow or orange to red by grinding–fuming and grinding–heating processes due to the morphological change from the thermodynamically stable crystalline phase to the metastable amorphous state. We are currently utilizing **1** as a fluorescent visualizer for tumor cell targeting and imaging. The details will be published in due course.

The work reported in this communication was partially supported by the National Science Foundation of China (20974028), the RPC and SRFI Grants of HKUST (RPC10SC13, RPC11SC09 and SRFI11SC03PG), the Research Grants Council of Hong Kong (604711, 603509, HKUST2/CRF/10 and N_HKUST620/11), the Innovation and Technology Commission (ITCPD/17-9) and the University Grants Committee of Hong Kong (AoE/P-03/08 and T23-713/11-1). B.Z.T. thanks the support from the Cao Guangbiao Foundation of Zhejiang.

Notes and references

1 (*a*) C. Weder, *J. Mater. Chem.*, 2011, **21**, 8235; (*b*) M. Wang, G. Zhang, D. Zhu and B. Z. Tang, *J. Mater. Chem.*, 2010, **20**, 1858; (*c*) H. Ito, T. Saito, N. Oshima, N. Kitamura, S. Ishizaka, Y. Hinatsu, M. Wakeshima, M. Kato, K. Tsuge and M. Sawamura, *J. Am. Chem. Soc.*, 2008, **130**, 10044.
2 (*a*) S. Jayanty and T. P. Radhakrishnan, *Chem.–Eur. J.*, 2004, **10**, 791; (*b*) H. J. Tracy, J. L. Mullin, W. T. Klooster, J. A. Martin, J. Haug, S. Wallace, I. Rudloe and K. Watts, *Inorg. Chem.*, 2005, **44**, 2003.
3 J. Luo, Z. Xie, J. W. Y. Lam, L. Cheng, H. Chen, C. Qiu, H. S. Kwok, X. Zhan, Y. Liu, D. Zhu and B. Z. Tang, *Chem. Commun.*, 2001, 1740.
4 (*a*) M. Levitus, K. Schmieder, H. Ricks, K. D. Shimizu, U. H. F. Bunz and M. A. Garcia-Garibay, *J. Am. Chem. Soc.*, 2001, **123**, 4259; (*b*) R. Deans, J. Kim, M. R. Machacek and T. M. Swager, *J. Am. Chem. Soc.*, 2000, **122**, 8565; (*c*) J. Huang, X. Yang, J. Wang, C. Zhong, L. Wang, J. Qin and Z. Li, *J. Mater. Chem.*, 2012, **22**, 2478; (*d*) J. Huang, N. Sun, J. Yang, R. Tang, Q. Li, D. Ma, J. Qin and Z. Li, *J. Mater. Chem.*, 2012, **22**, 12001.
5 (*a*) Y. T. Wu, M. Y. Kuo, Y. T. Chang, C. C. Shin, T. C. Wu, C. C. Tai, T. H. Cheng and W. S. Liu, *Angew. Chem., Int. Ed.*, 2008, **47**, 9891; (*b*) Z. Wang, H. Shao, J. Ye, L. Tang and P. Lu, *J. Phys. Chem. B*, 2005, **109**, 19627.
6 (*a*) Y. Li, F. Li, H. Zhang, Z. Xie, W. Xie, H. Xu, B. Li, F. Shen, L. Ye, M. Hanif, D. Ma and Y. Ma, *Chem. Commun.*, 2007, 231; (*b*) K. Kokado and Y. Chujo, *Macromolecules*, 2009, **42**, 1418; (*c*) M. C. Zhao, M. Wang, H. Liu, D. S. Liu, G. X. Zhang, D. Q. Zhang and D. B. Zhu, *Langmuir*, 2009, **25**, 676; (*d*) X. Xu, J. Huang, J. Li, J. Yan, J. Qin and Z. Li, *Chem. Commun.*, 2009, 12385.
7 For reviews, see (*a*) Y. Hong, J. W. Y. Lam and B. Z. Tang, *Chem. Soc. Rev.*, 2011, **40**, 5361; (*b*) Y. Hong, J. W. Y. Lam and B. Z. Tang, *Chem. Commun.*, 2009, 4332.
8 X. Wang, A. R. Morales, T. Urakami, L. Zhang, M. V. Bondar, M. Komatsu and K. D. Belfield, *Bioconjugate Chem.*, 2011, **22**, 1438.
9 A. Mishra, R. K. Behera, B. K. Mishra and G. B. Behera, *Chem. Rev.*, 2000, **100**, 1973.
10 B. J. Coe, J. A. Harris, J. J. Hall, B. S. Brunschwig, S.-T. Hung, W. Libaers, K. Clays, S. J. Coles, P. N. Horton, M. E. Light, M. B. Hursthouse, J. Garín and J. Orduna, *Chem. Mater.*, 2006, **18**, 5907.
11 X. Lv, J. Liu, Y. Liu, Y. Zhao, Y.-Q. Sun, P. Wang and W. Guo, *Chem. Commun.*, 2011, **47**, 12843.
12 F. Würthner, T. E. Kaiser and C. R. Saha-Möller, *Angew. Chem., Int. Ed.*, 2011, **50**, 3376.
13 (*a*) X. Luo, J. Li, C. Li, L. Heng, Y. Q. Dong, Z. Liu, Z. Bo and B. Z. Tang, *Adv. Mater.*, 2011, **23**, 3261; (*b*) Z. Chi, X. Zhang, B. Xu, X. Zhou, C. Ma, Y. Zhang, S. Liu and J. Xu, *Chem. Soc. Rev.*, 2012, **41**, 3878.
14 B. Zhu, F. Yuan, R. Li, Y. Li, Q. Wei, Z. Ma, B. Du and X. Zhang, *Chem. Commun.*, 2011, **47**, 7098.
15 (*a*) W. Qin, D. Ding, J. Liu, W. Z. Yuan, Y. Hu, B. Liu and B. Z. Tang, *Adv. Funct. Mater.*, 2011, **22**, 771.